Fermi National Accelerator Laboratory

FERMILAB-TM-1963

Field Shape of the Accumulator LDA Dipoles

Bruce C. Brown

Fermi National Accelerator Laboratory
P.O. Box 500, Batavia, Illinois 60510

May 1996

Operated by Universities Research Association Inc. under Contract No. DE-AC02-76CHO3000 with the United States Department of Energy

Disclaimer

This report was prepared as an account of work sponsored by an agency of the United States Government. Neither the United States Government nor any agency thereof, nor any of their employees, makes any warranty, expressed or implied, or assumes any legal liability or responsibility for the accuracy, completeness, or usefulness of any information, apparatus, product, or process disclosed, or represents that its use would not infringe privately owned rights. Reference herein to any specific commercial product, process, or service by trade name, trademark, manufacturer, or otherwise, does not necessarily constitute or imply its endorsement, recommendation, or favoring by the United States Government or any agency thereof. The views and opinions of authors expressed herein do not necessarily state or reflect those of the United States Government or any agency thereof.

Fermilab

Doc Number: TM-1963
Version: 1.2

Field Shape of the Accumulator LDA Dipoles

Bruce C. Brown
Accelerator Division/Main Injector Department
Fermi National Accelerator Laboratory *
P.O. Box 500
Batavia, Illinois 60510

5/8/96

Contents

1 Introduction **2**

2 Data Selection and Analysis **4**
2.1 Shape Calculation 6
2.2 Shape Errors 6
2.3 Initial Results 7
2.4 Exploring Limitations of Polynomial Fits 19
2.5 Additional Polynomial Fits 22

3 Results and Conclusions **26**

4 Acknowledgements **28**

A Measurement Hardware **30**

B Data Collection and Reduction **32**

C Effects of Fit Widths **34**

*Operated by the Universities Research Association under contract with the U. S. Department of Energy

Abstract

Large Aperture Dipoles (LDA) are used in the Fermilab Antiproton Accumulator to provide one half of the bending required for that storage ring. The production measurement data for those magnets are analyzed and the integrated field shape on the median plane at the design operating current (1180 A) is reported. When linear (quadrupole) and parabolic (sextupole) terms are subtracted, the remaining field errors are only $\sim 10^{-4}$ over a $\pm$ 4 inch aperture. Polynomial fits to that data can be interpreted in terms of normal harmonics of the magnetic field. However the polynomial fits are not unique. When the polynomial coefficients are expressed as harmonics with a reference radius of 1 inch, the nonlinear portions of this field (harmonics higher than quadrupole) are typically 10^{-5} to 10^{-6}. Both individual magnet results and statistical profiles are reported along with studies of the fitting limitations.

1 Introduction

The production measurement system for the dipoles in the TeV I project[1], which constructed the Fermilab AntiProton Source, used a FLATCOIL measurement[2][3] to study both the strength and shape of the integrated magnetic field. Data on each magnet was collected, analyzed, and reviewed during construction and the resulting data was utilized in the sorting algorithm used for placing magnets in the ring. The data has been stored, either on archive tapes or in VAX Indexed files for use in accelerator operations. However, no formal reports of these results have been available. In response to a need to provide field uniformity requirements for new storage ring design efforts, this report will make field uniformity information available on the LDA dipoles.

The LDA dipole design properties are described in the Tev I Project design report[1]. Each of these curved dipoles provides 15 ^{o} of bend for this 8 GeV proton storage ring. Using four of these dipoles at each of the three high dispersion regions of the lattice provides half of the bend required for the ring. The Accumulator is used to store beams over a very wide physical aperture, with an injection orbit on the outside, a core of stored beam on the inside and a "stack-tail" of beam being cooled extending between these orbits. This all takes place inside a vacuum chamber which is baked to provide ultra-high vacuum. Table 1 lists some relevant design features of the LDA dipoles. Since the core may be stored for days, the field uniformity requirements for it are demanding.

Length	180 inches
Sagitta	5.715 inches
Number	12 (+ 1)
Color	dark blue
Gap	2.375 inch
Nominal field	1.7 T
Weight	90,767 lbs.
Laminations	5918
Coil Turns	72
Conductor (copper) size	1×1.25 inch
Conductor Cooling Hole	0.375 inch dia.
Nominal current	1180 A
Resistance	20 mΩ
Inductance	234 mH
Power	28 kW
X Position of $\overline{P}$ Core	-2.492 inch
X Position of $\overline{P}$ Stacking Orbit	.579 inch
X Position of $\overline{P}$ Injection Orbit	3.161 inch
Vacuum Chamber Aperture (x)	$\pm$ 4.75 inch
Vacuum Chamber Aperture (y)	$\pm$ 0.75 inch

Table 1: Some LDA Dipole Parameters, mostly from the design report. Orbit positions are taken from Figure 5.3 and apply to those dipoles (half of them) at the largest dispersion.

Some details of the measurement hardware, software, and data collection procedures are given in Appendices A and B. Measurement runs produced data files which record flux changes produced by ramping the magnet at fixed position (baseline) or moving the probe at fixed excitation (scan). This report will describe the field shape measured in these magnets by combining results from data in these files. Parameters from polynomial fits to these shapes will be reported. Since accelerator design codes such as TEAPOT and MAD are to be used with this data, special efforts are made to prepare results as coefficients for a harmonics expansion of the field shape errors. For the rectangular geometry of the LDA magnet aperture, the natural fitting function is a product of hyperbolic and circular sinusoids in rectangular coordinates. A harmonic expansion is the solution to Laplace's Equation for cylindrical geometry and is only guaranteed to provide a convergent series within a circle of radius equal to the pole tip radius. We have explored the limitations of a polynomial fit to the scan data in order to provide useful harmonics for these magnets. To represent the measured deviations of the dipole field, we will use polynomial fits expressed as harmonics at a reference radius of 2.54 cm (1 inch) since that is characteristic of the vertical half aperture of the dipole and can be reasonably compared to a 5 or 10 σ of the beam size. Using available data, we can do this across a large portion of the aperture.

The discussion of polynomial fits to FLATCOIL data is probably more detailed than most readers will find of interest. This reflects the fact that FLATCOIL measurements have been used extensively at Fermilab MTF and suitable fitting has not been implemented. Explicit understanding of the limitations of the polynomial provides guidance in understanding previous efforts and future options. We hope uninterested readers can still locate the measurement results of interest.

2 Data Selection and Analysis

LDA data from the measurements taken in the B0 assembly hall (Test Stands E & F) have been available in a VAX indexed file to which all the 'REDuced' single run files have been 'swept'. Using the VAX DATATRIEVE program to manipulate this data (the B0FLATRED Domain), one representative scan run (measurement) was selected for each magnet. Where magnets had undergone extensive tests, including studies of re-assembly effects, later rather than earlier scan measurements were selected. In a similar fashion,

Magnet	Scan Run Date/Time	Baseline Run Date/Time	Points	Width	Loc
LDA001	22-Mar-1985 11:46:42.20	22-Mar-1985 12:21:59.33	67	4.95	A2B10
LDA002	6-Nov-1984 14:00:23.48	6-Nov-1984 14:25:17.98	61	4.5	A2B9
LDA003	25-Oct-1984 14:20:58.24	25-Oct-1984 13:57:30.92	46	4.5	A3B10
LDA004	12-Nov-1984 09:19:14.59	12-Nov-1984 09:43:16.47	61	4.5	A1B9
LDA005	26-Oct-1984 13:52:27.28	26-Oct-1984 13:32:28.81	46	4.5	A3B9
LDA006	28-Feb-1985 12:18:33.90	28-Feb-1985 12:45:10.51	65	4.8	A4B9
LDA007	23-Feb-1985 12:22:04.38	23-Feb-1985 12:47:46.17	65	4.8	A4B10
LDA008	1-Mar-1985 11:15:41.93	1-Mar-1985 11:40:50.67	65	4.8	A5B9
LDA009	25-Feb-1985 06:14:02.32	25-Feb-1985 06:40:45.13	65	4.8	A5B10
LDA010	25-Feb-1985 08:53:34.90	25-Feb-1985 09:25:28.26	65	4.8	A6B9
LDA011	1-Mar-1985 06:35:09.82	1-Mar-1985 07:07:10	65	4.8	A6B10
LDA012	23-Feb-1985 10:12:14.11	23-Feb-1985 10:39:06.58	65	4.8	A1B10
LDA013	8-May-1985 12:55:04.38	8-May-1985 12:41:53.89	61	4.5	Spare

Table 2: Scan and Baseline (normalization) runs used for Analysis. Variations in the step size (0.150 or 0.200 inch) and range of scans result in the variation in the number of data points. Scans are taken symmetrically to the range shown as Width. If there are an even number of points, no point is taken at $x = 0$. For convenience, we also shown the Accumulator location where each dipole was installed and is used.

one baseline run was selected for each scan, but the baseline runs to consider were limited to ones which corresponded to the same measurement program invocation (same hardware) and the same nominal current for measurement.

2.1 Shape Calculation

On a point by point basis, the shape data from the selected scan measurement was divided by the SLOPE from the corresponding selected baseline run to produce a normalized magnetic field shape. If we denote the integrated strength through the entire magnet length by $J(x) = \int B_y(x)dl$, then the relative shape is defined by $s(x) = \{J(x) - J(0)\}/J(0)$. The measurements record Flux per Ampere which is proportional to $J(x)/I$ and $\{J(x) - J(0)\}/I$. To reiterate, at each point the reduced scan run recorded the change *vs.* position in flux per ampere referenced to the x = 0 point. The baseline run recorded the change in flux per ampere in an excitation measurement sequence as the SLOPE. Using DATATRIEVE we then recorded for each magnet a file containing the reduced x position, the reduced shape normalized to the slope, $s(x)$, and the reduced shape error normalized to slope. Identifying information and some descriptive information on the data for each magnet is shown in Table 2.

2.2 Shape Errors

The errors reported with the reduced FLATCOIL data result from a particularly simple error treatment. The shape, $s(x)$, is the average of measurements taken on three passes of the scanning probe. The standard deviation of these answers is the reported error, which we normalize to produce the shape error, $se(x)$. The data are based on an integrated change in flux from the initial measurement point at the edge of the measured aperture. The correlation from point to point which is induced by the integration process is not accounted for by this error estimation procedure. The integrator drift correction also adds complexity to the estimate of measurement uncertainty. The correction used takes advantage of the fact that we measure the same real flux on each of the three passes. The observed flux change is given by the real flux change plus the offsets due to amplifier offset (integrator drift) and amplifier noise. The analysis uses a set of 10 points per pass, centered about the $x = 0$ position, to determine a drift correction which has terms with linear and quadratic time dependence. Since the dominant real error is amplifier noise, the drift correction sets this to zero near the center

of the scan. The resulting values of $se(x)$ increase approximately linearly about the $x = 0$ point, such that the graph of $se(x)$ *vs.* x looks like a 'V' with typical values at ± 4 inches being between $1 - 2 \times 10^{-5}$, depending upon measurement conditions. These error estimates are used in the PAW fitting routines, but they are clearly not a good representation of the actual measurement uncertainties.

Since we have used integration to produce our results, the results obtained will have a smoothness which belies the actual differential error. However, the actual magnetic fields also have a smoothness guaranteed by the distance between the magnetic sources and the measurement position. Since we average three traversals to produce our results, some of the false smoothness from integration will be eliminated. The actual point-to-point uncertainty will be apparent in the following plots. We see that unphysical steps in the data occur only rarely with an amplitude of 1×10^{-5} suggesting that the point to point uncertainty is a fraction of that size.

2.3 Initial Results

Physics Analysis Workstation (PAW) software was used for the subsequent analysis. The files produced by DATATRIEVE were read into PAW vectors with labels corresponding to the magnet serial number. Using these vectors, a number of results were obtained:

1. In Figure 1 we plot the shape data for all magnets. The error bars are as described above and in Appendix B and are an overestimate of the point-to-point error. Following the tradition of the TeV I magnet effort, we present Figure 2 in which the field nonuniformity due to quadrupole fields is removed, allowing an expanded scale on which to view the dominant sextupole error and to observe the deviations from that. Since sextupole correctors are available to correct the Accumulator operation, we consider observing the nonuniformity on a finer scale by displaying the same scan data but this time subtracting both the average quadrupole and average sextupole term from the data. This is illustrated in Figure 3.

2. Using sliding data windows, polynomial fits (PAW P7 function which includes terms to x^7) to the data regions are used to extract coefficients which are then interpreted as normal harmonics[4] *vs.* position

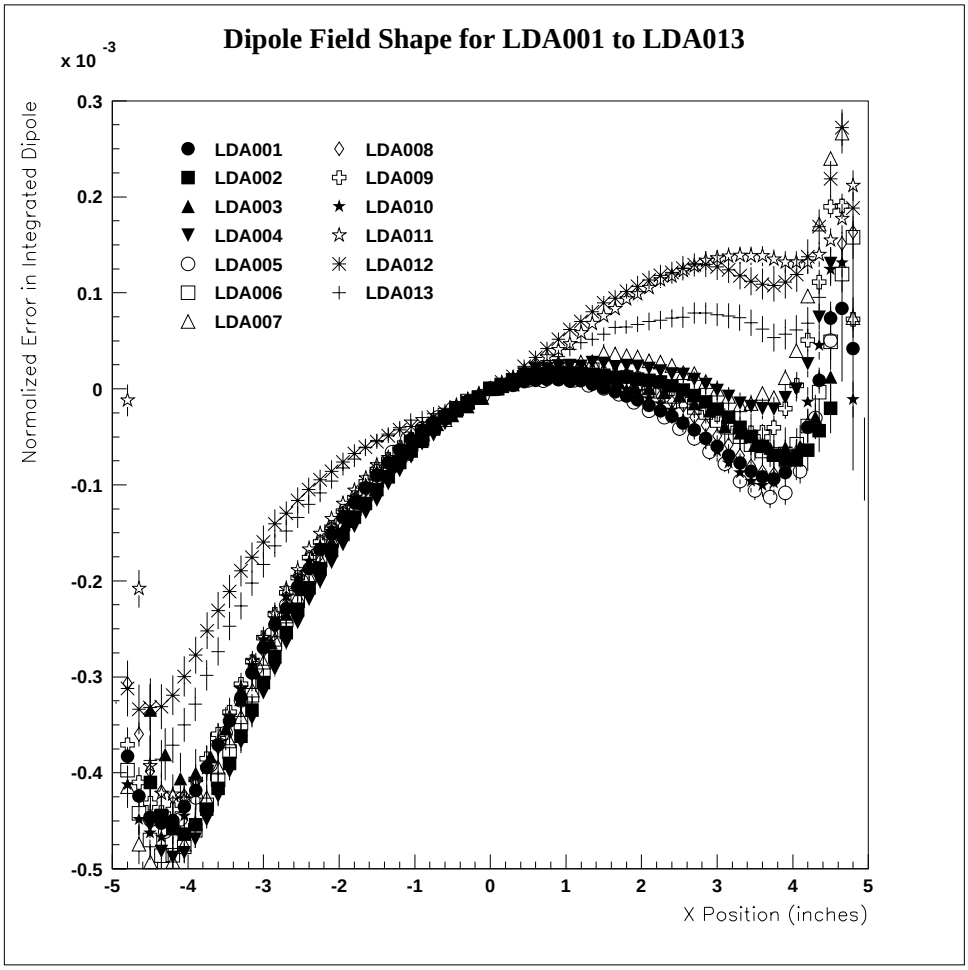

Figure 1: Deviation of integrated dipole field from value at $x = 0$ as measured using a FLATCOIL scan. These are quantities $s(x)$ with error bars $se(x)$ as defined in the text.

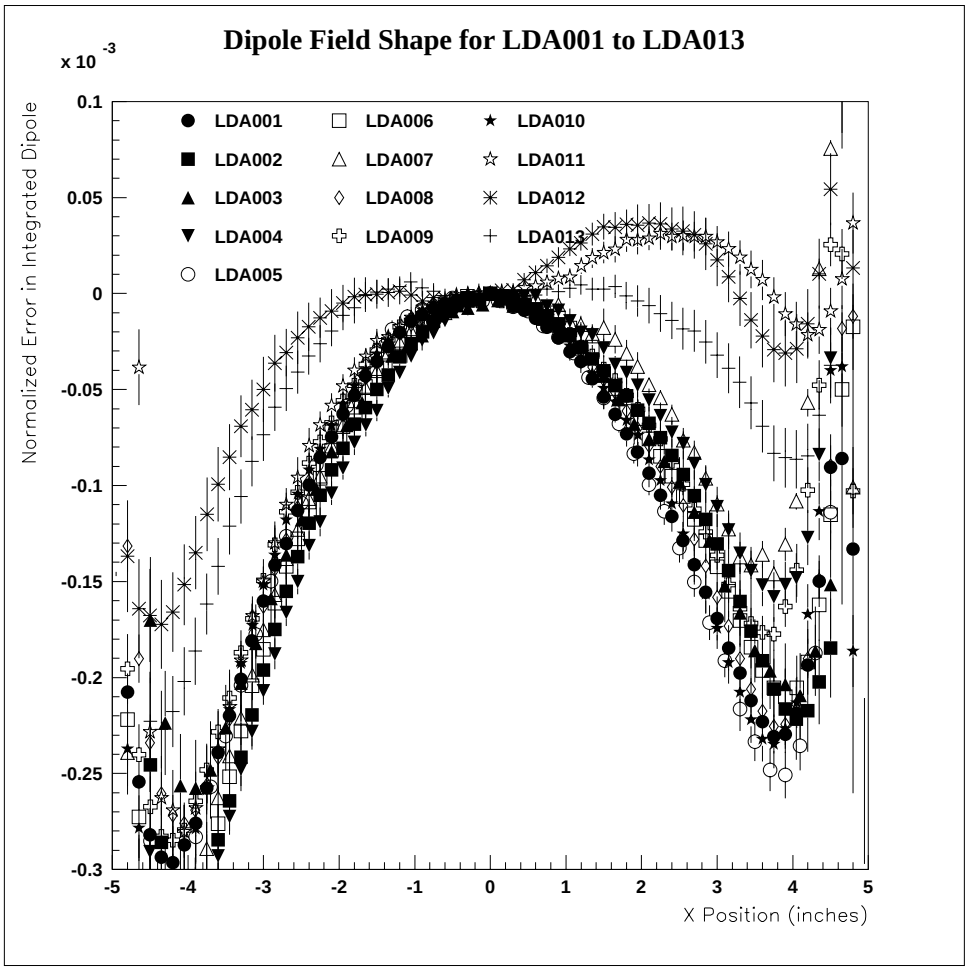

Figure 2: Scan data from previous plot with quadrupole term subtracted, $s(x) - < b_2 > x$. For this purpose the average quadrupole at $x = 0$ for first 10 magnets using a fit width of ± 1 inch was used.

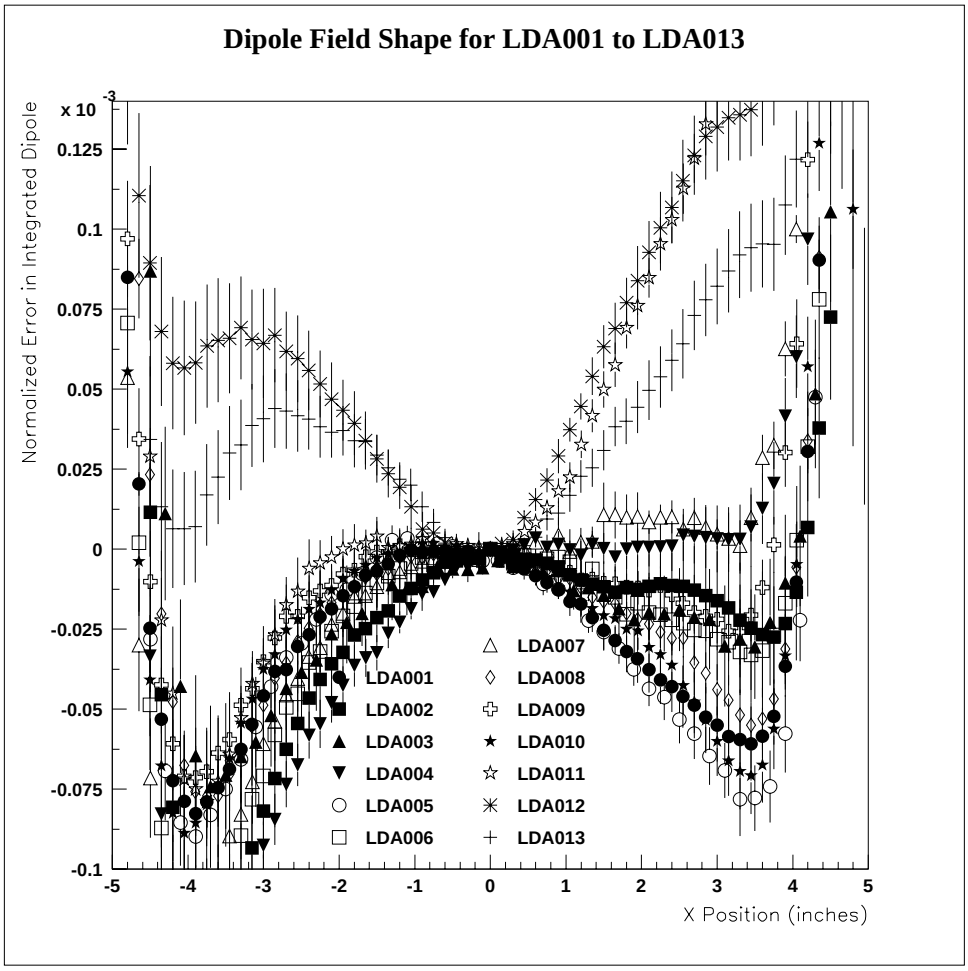

Figure 3: Scan data from previous plot with quadrupole and sextupole term subtracted, $s(x) - < b_2 > x - < b_3 > x^2$. The average quadrupole and sextupole at $x = 0$ for first 10 magnets using a fit width of ± 1 inch was used.

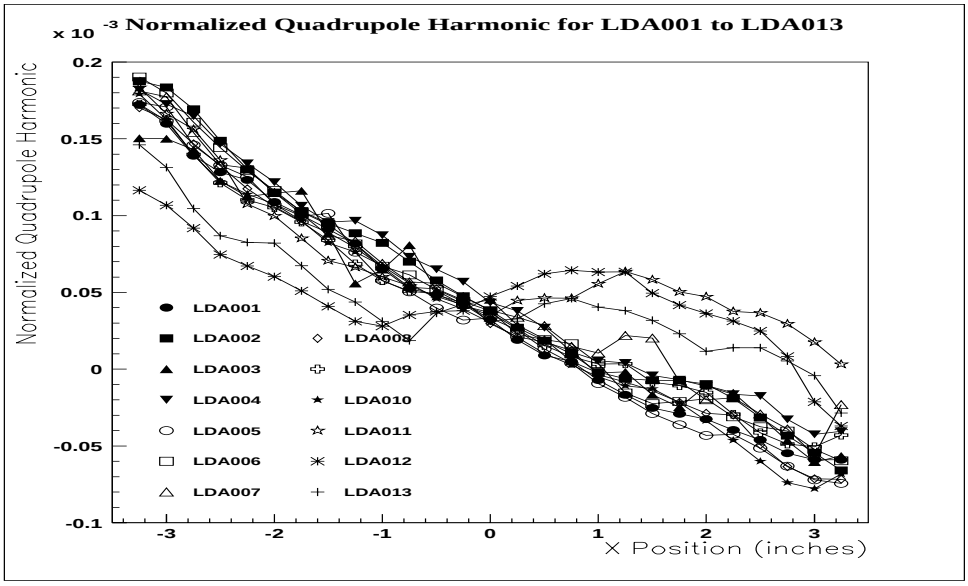

Figure 4: Local Quadrupole, b_2, from fit to region ± 1 inch wide centered on plotted point, x_p. Fit is to the form $s(x) = b_1 + b_2(x - x_p) + b_3(x - x_p)^2 + \cdots$

up to 16-pole with a reference radius of 1 inch (25.4 mm).[1] The representation used is express by

$$\int B_y(x, y=0, z)dz = \left(\int B_y(x=0, y=0, z)dz\right)[1 + b_2 x + b_3 x^2 + \cdots] \tag{1}$$

with x in inches. The window algorithm for data selection consists of using one data point beyond a fixed window size (to account for the variation in step size among measurements). In Figure 4 and 5 we plot quadrupole and sextupole results for a window size of ± 1 inch with the window moving 0.25 inches per step. This is the largest range which can be accommodated for the complete data set.

[1] We refer to harmonics of a magnetic field as coefficients of a fit in cylindrical coordinates for a field in which there is no variation in the third (z) dimension. We normalize to the field of the dominant component (dipole in this case) at a reference radius to obtain normalized harmonics. The terms normal (b_n) and skew (a_n) harmonics refer to the cosine-like and sine-like terms where the skew components do not contribute to B_y along the x axis.

x(inches)	-3.0	-2.0	-1.0	0.0	1.0	2.0	3.0
Magnets LDA001 thru LDA010							
$< b_2 >$	1.680	1.118	0.685	0.365	-0.006	-0.223	-0.596
σb_2	0.104	0.055	0.094	0.052	0.062	0.115	0.110
$< b_3 >$	-0.282	-0.213	-0.162	-0.174	-0.153	-0.088	-0.083
σb_3	0.075	0.124	0.132	0.068	0.123	0.102	0.127
$< b_4 >$	-0.268	0.064	0.085	-0.079	0.144	-0.068	0.268
σb_4	0.217	0.137	0.166	0.219	0.168	0.255	0.324
$< b_5 >$	0.167	0.013	-0.114	0.013	0.016	-0.119	0.227
σb_5	0.126	0.242	0.284	0.156	0.191	0.131	0.152
$< b_6 >$	0.202	-0.120	-0.127	0.127	-0.213	0.059	0.101
σb_6	0.458	0.264	0.260	0.385	0.257	0.412	0.509
$< b_7 >$	-0.008	-0.031	0.086	-0.010	-0.009	0.064	-0.014
σb_7	0.074	0.132	0.160	0.093	0.092	0.064	0.103
$< b_8 >$	-0.118	0.075	0.075	-0.060	0.100	-0.023	-0.045
σb_8	0.234	0.133	0.141	0.194	0.112	0.208	0.255
Magnets LDA001 thru LDA013							
$< b_2 >$	1.603	1.046	0.618	0.368	0.118	-0.099	-0.465
σb_2	0.211	0.165	0.167	0.057	0.246	0.268	0.279
$< b_3 >$	-0.290	-0.208	-0.149	-0.127	-0.113	-0.094	-0.153
σb_3	0.077	0.108	0.142	0.125	0.138	0.090	0.183
$< b_4 >$	-0.212	0.001	0.095	-0.006	0.117	-0.044	0.216
σb_4	0.266	0.184	0.163	0.259	0.155	0.251	0.326
$< b_5 >$	0.124	0.000	-0.075	0.020	-0.005	-0.083	0.240
σb_5	0.171	0.219	0.304	0.167	0.172	0.134	0.183
$< b_6 >$	0.138	-0.007	-0.112	0.023	-0.210	0.058	0.066
σb_6	0.575	0.325	0.285	0.433	0.228	0.403	0.464
$< b_7 >$	0.012	-0.022	0.057	-0.014	0.003	0.038	-0.024
σb_7	0.088	0.123	0.180	0.096	0.082	0.075	0.109
$< b_8 >$	-0.084	0.021	0.063	-0.015	0.101	-0.036	-0.016
σb_8	0.295	0.159	0.165	0.213	0.101	0.205	0.232

Table 3: Average and RMS of results from polynomial fits expressed as normal harmonics at a reference radius of 1 inch. A factor of 10^{-4} has been suppressed so results are in "Standard Units". Fits were performed at positions shown with a nominal 1 inch range of x values (see description of point selection above) and using a polynomial with terms up to x^7. Measurements were taken at spacings of 0.150 or 0.200 inches. Since LDA's are not sector magnets, they have an end quadrupole term which is not measured by FLATCOIL and is not shown here.

3. Using the fitted data in Item 2 above, we find the mean and standard deviation of the harmonic fits for the thirteen magnets and separately for magnets 001 through 010 which are more uniform. These statistical properties are also reported in Table 3 at a limited number of positions. These results are plotted in Figures 6, 7, and 8. Since only data on the median plane is used for these fits, the harmonic representation is equivalent to the ordinary polynomial which was used for these fits. It does not provide an orthogonal set for fitting and high order terms are sensitive to the number of fitting terms used which adds a systematic uncertainty to their interpretation. (See below).

4. The desire to fit all of the magnets for averaging restricted the fit parameters and even the fit range to match to lowest common denominator. In order to observe the fit shape over the widest possible range, we examine the data for LDA001. Finding a suitable compromise between fit range and smoothness of fit results (taken as an indicator of fit quality) requires some exploration. It was observed that where the field is quite non-uniform, the precision of the fit is less critical. With

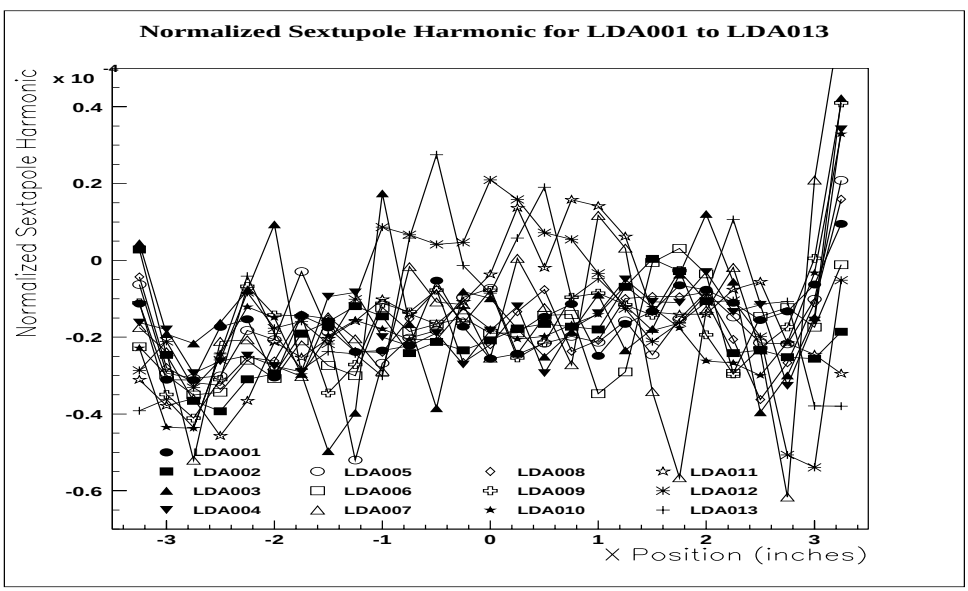

Figure 5: Local Sextupole, b_3, from fit to region ± 1 inch wide centered on plotted point, x_p.

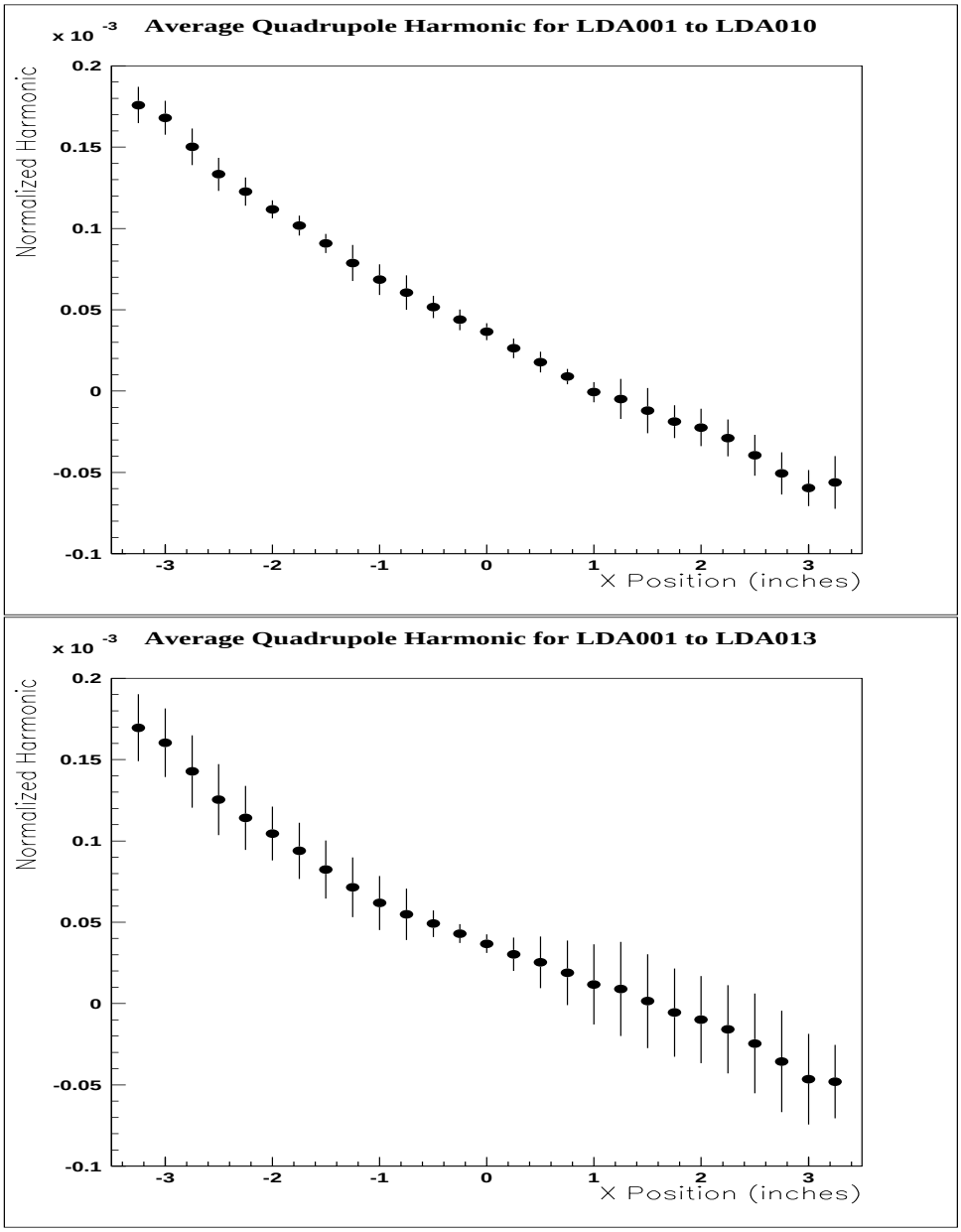

Figure 6: The average quadrupole *vs.* position is plotted for selected (above) and all (below) LDA dipoles. The error bars represent the standard deviation for the selected magnet set.

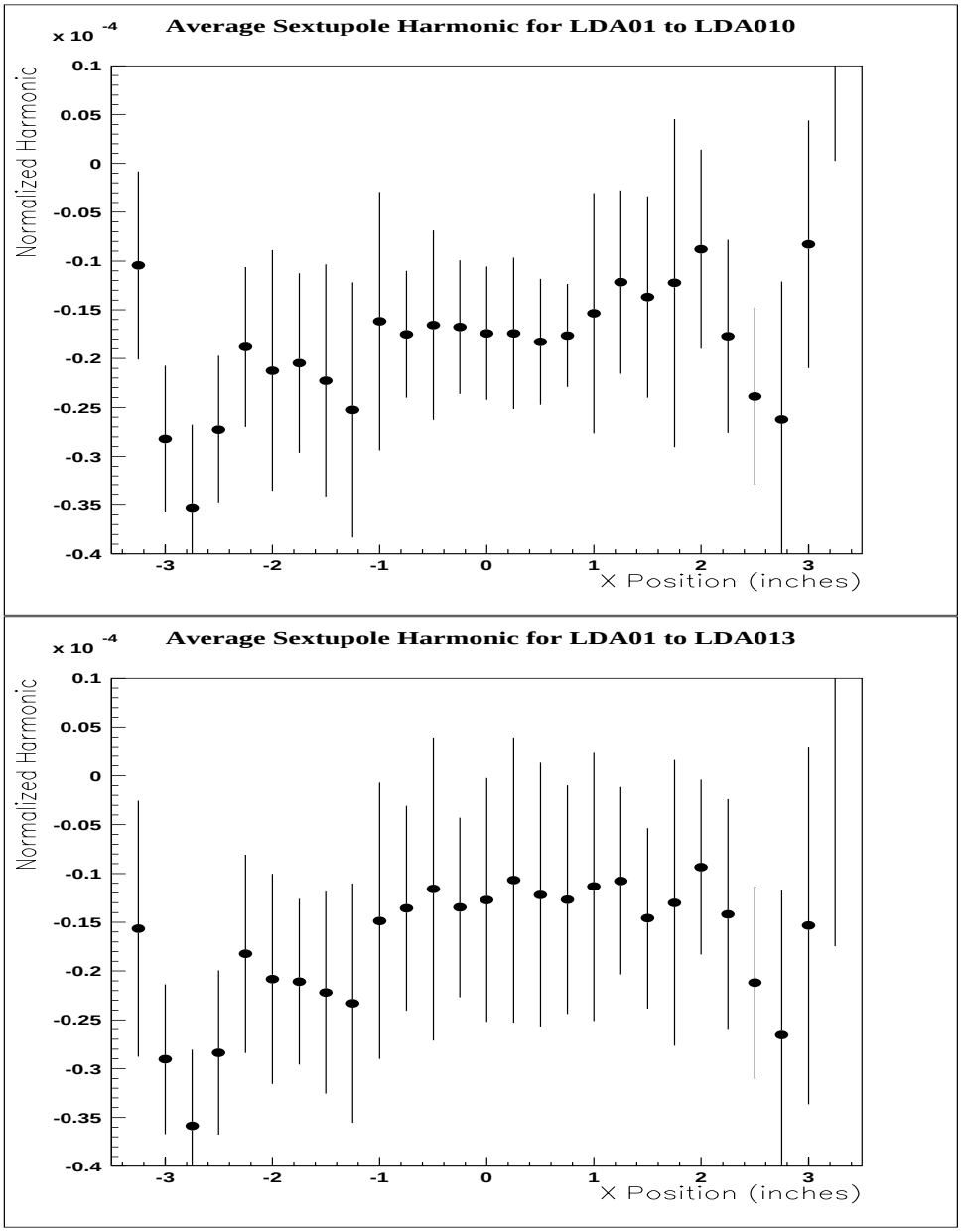

Figure 7: The average sextupole *vs.* position is plotted for selected (above) and all (below) LDA dipoles. The error bars represent the standard deviation for the selected magnet set.

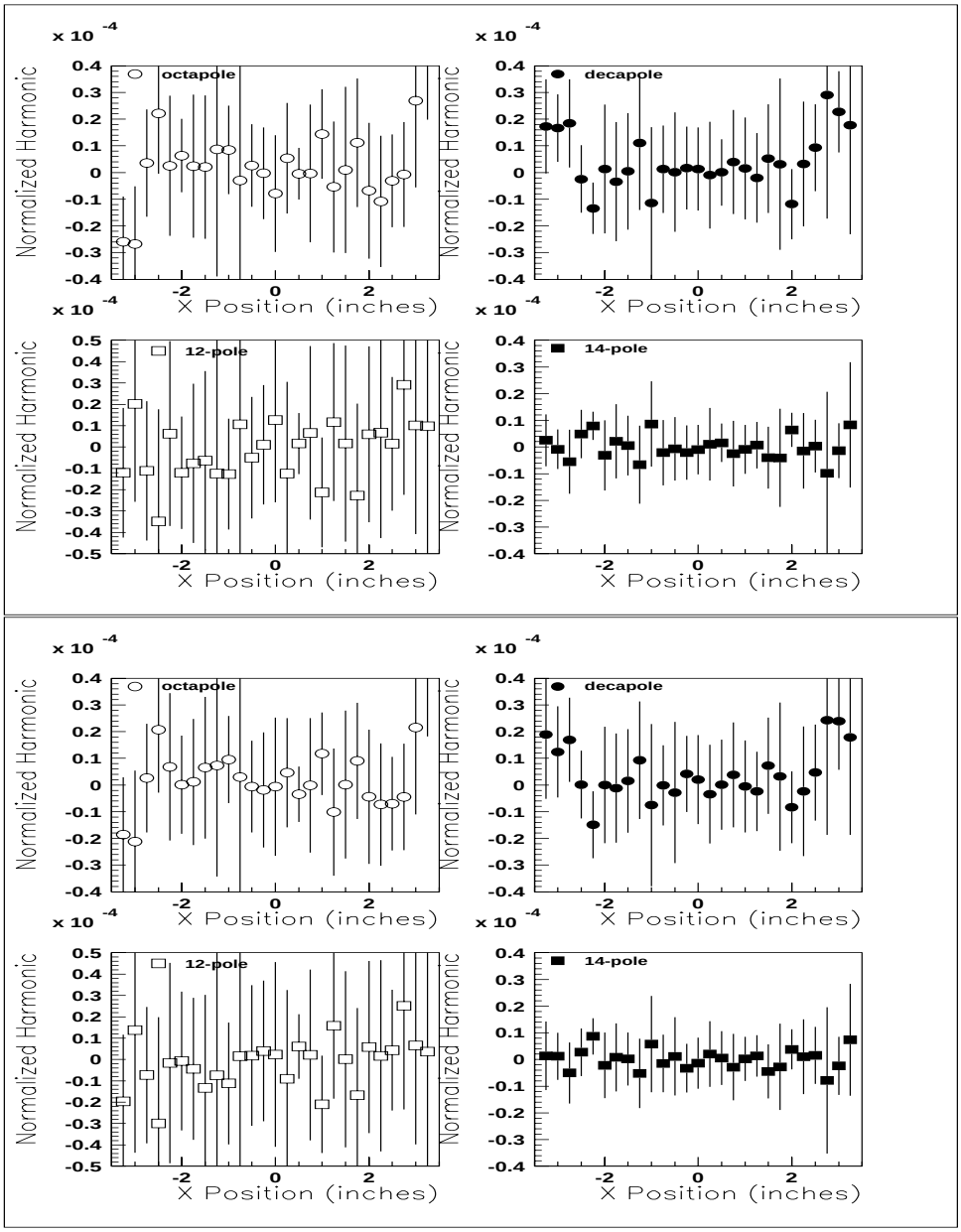

Figure 8: The average multipole value *vs.* position is plotted for selected (above) and all (below) LDA dipoles. The error bars represent the standard deviation for the selected magnet set.

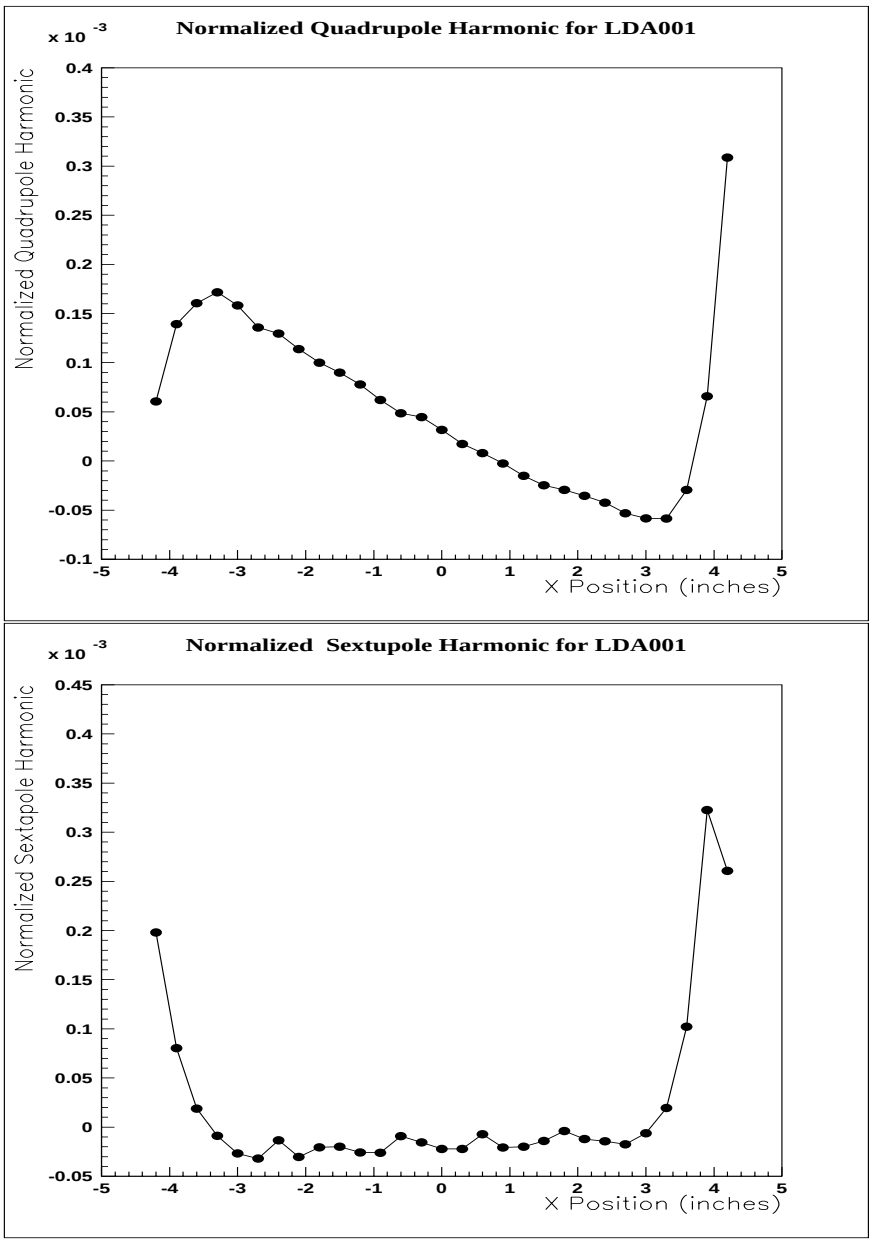

Figure 9: Scan data fit to a polynomial with results expressed as normal quadrupole (above) and normal sextupole (below) normalized harmonics. These fits used polynomial terms up to x^5 and a fit width of 0.75 inches with fits performed every 0.3 inches.

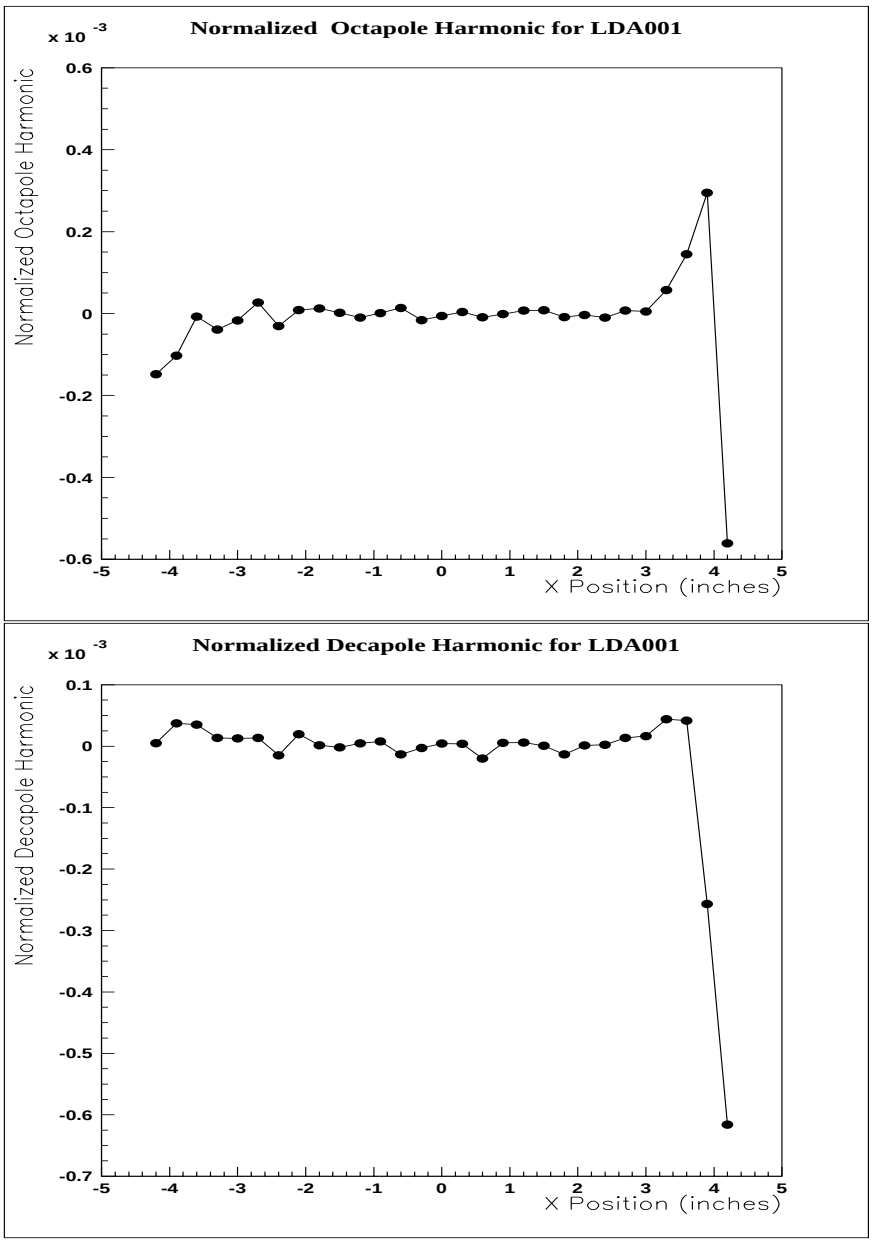

Figure 10: Scan data fit to a polynomial with results expressed as normal octapole (above) and normal decapole (below) normalized harmonics. These fits used polynomial terms up to x^5 and a fit width of 0.75 inches with fits performed every 0.3 inches.

that in mind, we choose a fit using terms up to x^5 (PAW P5 polynomial) and a fit width of 0.75 inches which permit directly presenting the harmonic values beyond the radii of the core or the injection orbit. In fact, for these measurements, the coil centerline scanned beyond the current location of the vacuum chamber wall, and the fit results extend nearly to that location. The results are shown in Figures 9 and 10.

2.4 Exploring Limitations of Polynomial Fits

The general procedure used in obtaining magnetic field properties is to acquire an over-determined (for the proposed fitting function) set of measurement data (*e.g.* flux *vs.* position) with some measurement system. After correcting for any system limitations which can be removed on a point by point or run by run basis, one fits the measured values to a suitable function, thereby determining some parameters which will be used to characterize the magnetic field. The appropriate function depends upon the field geometry, the coil geometry, probe motion geometry and data acquisition sequence. The polynomial fitting described above[2] has two areas of concern in this regard.

- As noted above, the errors attached to the measured points are not well behaved, over-estimating the errors over much of the range and perhaps underestimating the errors at small x. This effect is not likely to be critical, but it makes it more difficult to assess fit quality. In addition, fits might be more appropriately constrained, expecially for small fit ranges, if accurate error estimates could be used.

- When fitting to functions which are guaranteed to provide convergent fits to the data over available ranges, one can use the over-constrained data with the proper fitting function to eliminate anomalies in the measured data using constraints provided by the fitting function. When using a possibly divergent series, one loses this constraint on the fitting process.

[2]Since we only have measured the field on the median plane at a series of positions, the polynomial fit is equivalent to (describes the data as well as) any other representation of the data we can obtain. An orthonormal set of polynomials might remove some of the arbitrariness in fit order and range, but there is no fundamental relation between them and the field in the volume. The ordinary polynomials which were used have a useful relation to the harmonic representation which is applicable over a cylindrical volume of the magnet gap. If we first fit to an orthonormal polynomial and then re-expressed the results in terms of ordinary polynomials, information would be lost from the fit.

In this problem, we would be well served by measurements at other y values to further constrain the measurements. These limitations to the selected FLATCOIL measurement system were not unfamiliar to the system designers, but cost and mechanical robustness considerations, as well as the adequacy of the data obtained, encouraged the system design which was adopted. Of course, representations other than a harmonic expansion would serve well with this data, but the desire to provide input which is traditional for the Accelerator simulation codes has caused us to attempt to produce the traditional results.

In Appendix C, we review the data which demonstrates that the degree to which quadrupole and sextupole terms can be removed, leaving only high order contributions to the field, depends in detail upon the scan range used for the fitting. The fact that the sextupole determined for each magnet using a 1 inch fit width was a poorer representation of its behavior at large x than was the 10 magnet average, suggested that the fitting was not optimal, probably being limited by the measurement errors for narrow widths. We simultaneously discovered that the RMS of the harmonic values obtained even with only an increase to 1.5 inch fit widths were typically 3 to 10 times smaller than those fit with 1 inch fitting range. This appeared to be an unsatisfactory point to stop analysis.

It was recognized at this point that the fundamental limitations of using polynomial fits rather than functions which solved the Laplace Equation for the geometry in question would impact the ultimate fitting options, however, it was not known what practical boundaries existed for the data at hand. Two studies were used to gain insight into the possibilities for polynomial fits.

Is it possible to select fitting widths and number of polynomial terms to provide an optimal fit for low order harmonics? Using a series of plots such as Figure 11, this was explored for polynomials from P5 to P14. Two general features of these fits become apparent.

- If we attempt to use only a few (low order) terms, the low order harmonics are distorted at high fit widths. We see this for the P7 fit to sextupole above 3.5 inches. The P6 fits (not shown) have a similar effect, while the sextupole becomes more negative at high fit widths with the P5 fits (also not shown).

- At low fit widths, the high order terms depend strongly on the fit width chosen. Note this in both the mean and especially the standard

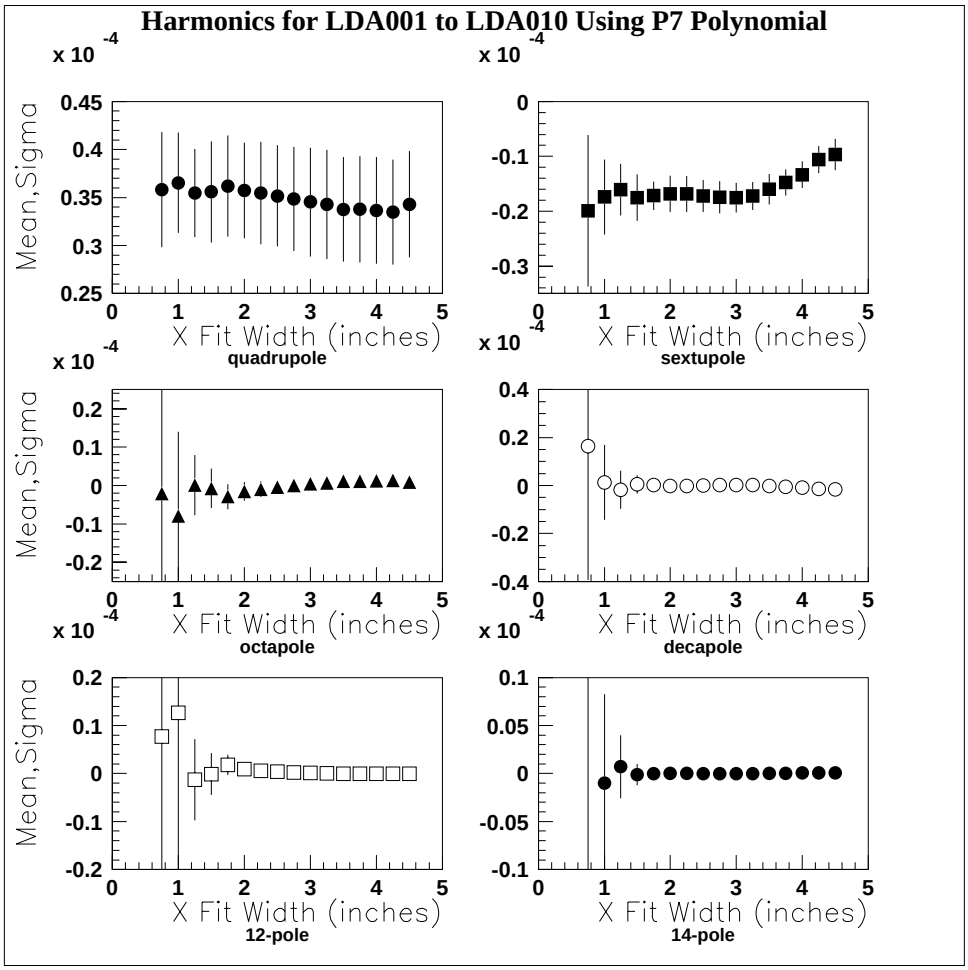

Figure 11: Mean (point) and standard deviation (error bars) for polynomial coefficients expressed as normalized harmonics. Fits are about $x = 0$ with results plotted *vs.* the fit width.

deviation for 12-pole and 14-pole. But even the octapole and decapole terms are not stable at low fit widths.

For low fit widths, the highest order terms grow to match small measured deviations using small differences of sets of much larger terms with the same symmetry (odd or even). This phenomenon most strongly affects the lowest widths and highest harmonics. However, even for P7, we see it out to 1.5 inch width for 12-pole. It is likely responsible for the large RMS of the sextupole with a fit width of 0.75 inches. This plot clearly shows that the RMS values and to a lesser extent the mean values in Table 3 would be quite different with a wider fit width (see additional fits below).

To gain further insight into the convergence problems, one can examine Figure 12. Here we have re-expressed the harmonics using a reference radius of $4''$, in order to see the contributions of all the terms at this larger radius. Returning to Figure 3 we see that the actual deviations are of order of magnitude 10^{-4}. To fit these deviation with the P18 polynomial, terms of even symmetry have amplitudes of order 10^{-1} with signs such that the differences of these large numbers produce the fitted shape. Terms of odd symmetry are $\times 50$ smaller. The quadrupole and sextupole terms have mean values which are large compared to their RMS spread. Additional plots were examined which showed that the mean and RMS of the higher order polynomial coefficients fell exponentially *vs.* the fit width at a fixed fit order. Thus, in dramatic fashion, we see illustrated a non-convergent series[3].

In reviewing all of the polynomials considered, we find that P5 will be suitable for most harmonics with fit widths between 1.25 and 3 inches, however, it does not contain a 14-pole term. High order fits permit wide fit ranges without distortion, however, narrow fit ranges have unacceptable variations of both mean and RMS which demands, for example, more than $2''$ of fit width for sextupole and $2.5''$ for 14-pole when using the P12 polynomial. The mathematician's warning about convergence is born out.

2.5 Additional Polynomial Fits

Using the procedures developed for the above studies, we obtain additional results by specifying the desired input parameters to the PAW Macros. Table 4 presents, as does Table 3, the average (and standard deviation of)

[3] We mean the series of fits, not the series of terms in the fit, as normally intended in the mathematical sense of convergence.

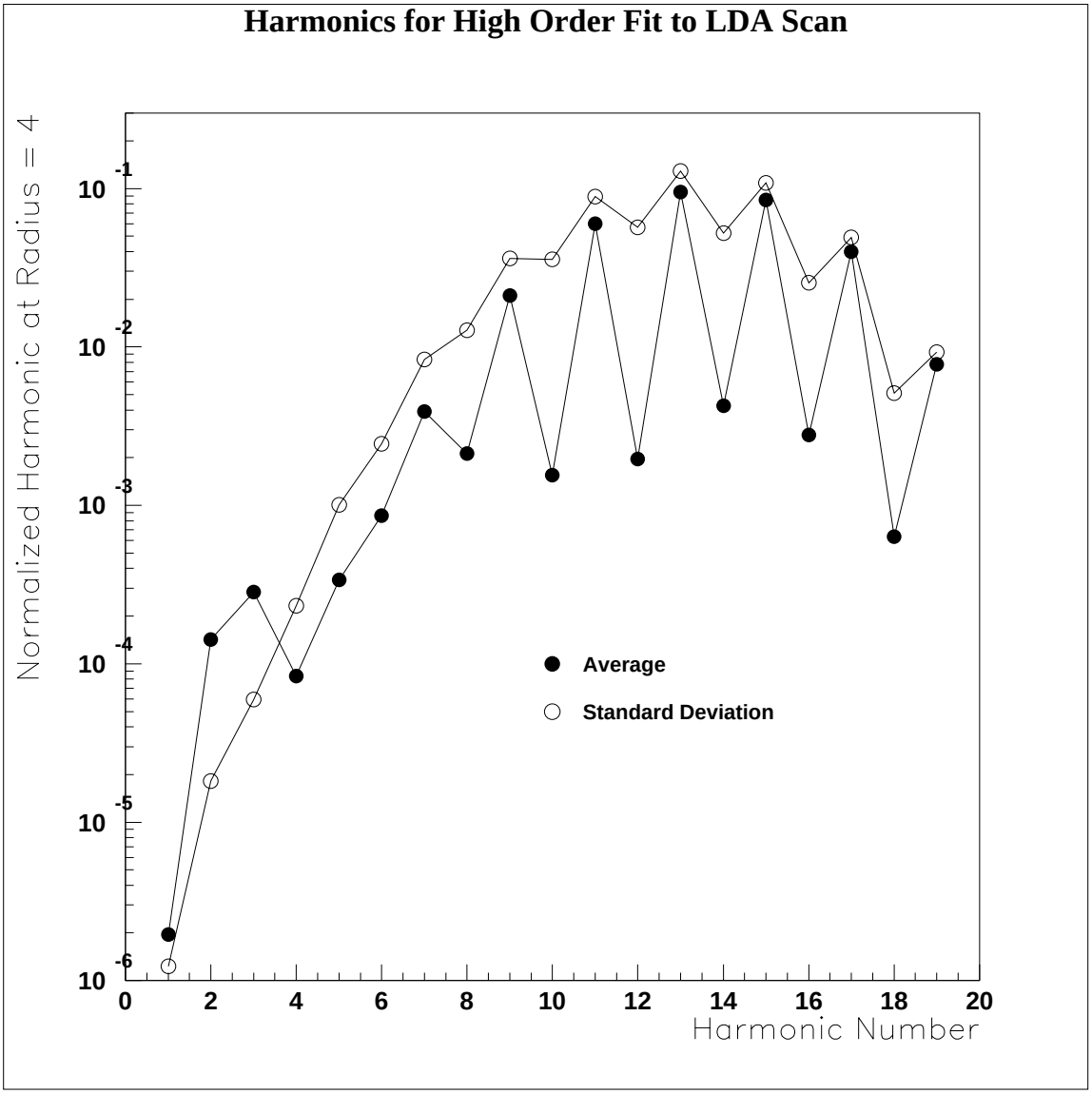

Figure 12: Using a polynomial fit with a fit width of 4.5″, the mean (solid) and standard deviation (open) for polynomial coefficient amplitudes expressed as normalized harmonics are shown. Fits are about $x = 0$ with results plotted *vs.* harmonic number for a P18 fit. For this plot only, the reference radius was set to 4″ to permit a comparison of the contributions of the various terms near the aperture limit.

x(inches)	-3.0	-2.0	-1.0	0.0	1.0	2.0	3.0
Magnets LDA001 thru LDA010							
$< b_2 >$	1.653	1.123	0.687	0.356	0.011	-0.225	-0.561
σb_2	0.114	0.054	0.083	0.053	0.072	0.102	0.113
$< b_3 >$	-0.278	-0.201	-0.204	-0.175	-0.149	-0.119	-0.175
σb_3	0.068	0.043	0.049	0.042	0.058	0.074	0.113
$< b_4 >$	-0.093	0.006	0.049	-0.007	0.019	-0.045	0.122
σb_4	0.099	0.096	0.066	0.051	0.044	0.093	0.217
$< b_5 >$	0.152	-0.040	0.012	0.005	0.002	-0.039	0.349
σb_5	0.048	0.031	0.038	0.038	0.035	0.040	0.196
$< b_6 >$	-0.076	0.014	-0.028	-0.001	0.004	0.008	0.214
σb_6	0.092	0.062	0.040	0.044	0.039	0.075	0.221
$< b_7 >$	0.003	0.012	-0.004	-0.001	-0.001	0.014	-0.044
σb_7	0.011	0.007	0.009	0.011	0.007	0.009	0.055
$< b_8 >$	0.007	-0.005	0.006	0.002	-0.002	0.003	-0.047
σb_8	0.023	0.013	0.009	0.010	0.010	0.019	0.058
Magnets LDA001 thru LDA013							
$< b_2 >$	1.579	1.042	0.621	0.367	0.135	-0.101	-0.436
σb_2	0.229	0.180	0.162	0.056	0.248	0.260	0.270
$< b_3 >$	-0.303	-0.201	-0.176	-0.124	-0.117	-0.114	-0.216
σb_3	0.077	0.048	0.073	0.108	0.086	0.065	0.129
$< b_4 >$	-0.067	0.010	0.067	0.006	-0.011	-0.015	0.087
σb_4	0.124	0.091	0.079	0.054	0.072	0.098	0.217
$< b_5 >$	0.146	-0.039	0.007	0.005	0.000	-0.038	0.313
σb_5	0.055	0.031	0.034	0.033	0.033	0.041	0.189
$< b_6 >$	-0.079	0.012	-0.033	-0.006	0.010	-0.013	0.187
σb_6	0.082	0.057	0.043	0.040	0.040	0.077	0.202
$< b_7 >$	0.003	0.012	-0.002	-0.002	0.000	0.013	-0.037
σb_7	0.011	0.007	0.009	0.010	0.006	0.010	0.051
$< b_8 >$	0.007	-0.004	0.007	0.003	-0.003	0.006	-0.039
σb_8	0.021	0.012	0.009	0.009	0.010	0.018	0.054

Table 4: Average and RMS of results from polynomial fits expressed as normal harmonics at a reference radius of 1 inch. A factor of 10^{-4} has been suppressed so results are in "Standard Units". Fits were performed at positions shown with a 1.5 inch range of x values (see description of point selection above) and using a polynomial with terms up to x^7. Measurements were taken at spacings of 0.150 or 0.200 inches. Since LDA's are not sector magnets, they have an end quadrupole term which is not measured by FLATCOIL and is not shown here.

Polynomial	P5	P6	P7	P8	P9	P5	P6	P7
Fit Center	-2.5	-2.5	-2.5	-2.5	-2.5	-2.5	-2.5	-2.5
Fit Width	1.0	1.0	1.0	1.0	1.0	1.5	1.5	1.5
Magnets LDA001 thru LDA010								
$< b_2 >$	1.353	1.352	1.333	1.333	1.326	1.359	1.358	1.351
σb_2	0.100	0.100	0.102	0.106	0.118	0.089	0.089	0.103
$< b_3 >$	-0.301	-0.278	-0.273	-0.262	-0.275	-0.307	-0.286	-0.287
σb_3	0.036	0.072	0.075	0.149	0.161	0.050	0.066	0.067
$< b_4 >$	0.062	0.063	0.222	0.222	0.322	0.048	0.050	0.074
σb_4	0.107	0.104	0.226	0.238	0.632	0.026	0.025	0.081
$< b_5 >$	0.051	-0.006	-0.024	-0.067	0.008	0.053	0.028	0.030
σb_5	0.046	0.103	0.127	0.550	0.590	0.021	0.042	0.042
$< b_6 >$	-0.037	-0.039	-0.349	-0.350	-0.751	-0.033	-0.034	-0.054
σb_6	0.077	0.076	0.526	0.536	2.269	0.008	0.007	0.059
$< b_7 >$		0.035	0.049	0.109	-0.025		0.007	0.006
σb_7		0.078	0.090	0.755	0.819		0.009	0.010
$< b_8 >$			0.171	0.172	0.755			0.005
σb_8			0.335	0.340	2.966			0.013
Magnets LDA001 thru LDA013								
$< b_2 >$						1.279	1.278	1.272
σb_2						0.208	0.208	0.208
$< b_3 >$						-0.309	-0.285	-0.286
σb_3						0.062	0.071	0.072
$< b_4 >$						0.052	0.054	0.075
σb_4						0.029	0.030	0.074
$< b_5 >$						0.048	0.021	0.022
σb_5						0.029	0.045	0.046
$< b_6 >$						-0.031	-0.032	-0.049
σb_6						0.010	0.010	0.057
$< b_7 >$							0.007	0.007
σb_7							0.009	0.010
$< b_8 >$								0.004
σb_8								0.012

Table 5: Average and RMS of results from polynomial fits expressed as normal harmonics at a reference radius of 1 inch. A factor of 10^{-4} has been suppressed so results are in "Standard Units". Fits were performed at positions, fit width and polynomial shown. Since LDA's are not sector magnets, they have an end quadrupole term which is not measured by FLATCOIL and is not shown here. $x = -2.5$ inch is the design position of the $\overline{P}$ Core.

harmonic components for polynomial fits at $1''$ intervals across the magnet aperture using a fit width of $1.5''$ (instead of the $1''$ used for Table 3).

Table 5 provides fits about $-2.5''$ which is near the location of the high density core of anti-protons in the Accumulator for those magnets at the high dispersion locations (A1B10, A2B10,...A6B10). Alternative polynomial order and fit widths as well as choices between 10 and 13 magnet averages are provided.

We have examined the the fit quality and find that the fitted curves do fit to the measured points with accuracy which matches the irregularities of the data. Since there is no 'best' fit, we have given several. Since the apparent errors are much smaller for the fits using 1.5 inch wide data groupings, they may be preferred, but that choice is left to the user of this data. Individual tables of magnet parameters are not presented, but can be printed from PAW after executing the macros used to produce these results.[4]

3 Results and Conclusions

This analysis has the principal goal to establish the field shape errors (deviations from uniform dipole field) and their variation from magnet to magnet among the LDA dipoles. In light of the very small field errors in each magnet (Figures 1, 2, 3) and the small variation from magnet to magnet as shown in the results tables, some care has been required to discover how the measurement data and analysis procedures contribute to the variations reported.

Examination of the field shape measurements is facilitated by the suppression of quadrupole and sextupole terms as in Figure 3. After examining all of the available data for this study one can pick out the anomalies in the data plotted there. Field variations are governed by the size scales in magnet. For LDA dipoles, the gap and the coil dimensions define these scales. Thus, we know that variations over a single measurement step (0.15 or 0.20

[4]The data on LDA's is stored in the original VAX format on both MDTF00 and ALMOND VAX clusters. To access it with DATATRIEVE, locate the DOMAIN CDD$TOP.MSR.PROD.FC$DATA.B0FLATRED. This points to either for the following files: MDTF00::TEVIREDROOT:[DATAFILE]B0FLATRED.DAT or ALMOND::USR$DISK4:[MDTFCZAR.TEVIDATA]B0FLATRED.DAT. This analysis has been carried out mostly using tools available on the MDTF Sun computers. Access to the data used and the macro's which processed it is possible by beginning with the file /usr/analysis/LDA/aaareadme.txt and examining the files, located in the same directory, which are described there.

inches) which do not smoothly match the scale of nearby changes are the result of a measurement system problem. We can pick out one such problem for LDA007. It appears as a step at 1.5 inch in the field shape plot or as a bump between 1.0 and 1.5 inches in the gradient plot. This bump is about 10^{-5} in relative field strength. In general, the plots are smoother than that, indicating that the overall shape measurement provides answers with a resolution of a few parts per million. Minor variations in measurement quality over the many months of operation are also seen but no trend is obvious.

We believe that the polynomial fits above are of use in describing the magnetic fields of these magnets. For issues where the differences between higher order harmonic terms (higher than the sextupole), as determined with 1 inch *vs.* 1.5 inch fit widths, are important, then either a different fitting procedure or at least the use of the individual magnet data may be required. However, since we have no measure of the skew fields for these magnets, we doubt that quantitative studies which depend upon higher order multipoles will find the details of these measurements to be sufficient. The present effort was only intended to set a scale for the non-uniformities.

The symmetry properties of magnets normally provide a hierarchy in the harmonic values – the symmetry allowed values are largest except when specifically suppressed by design geometry, next smaller are symmetry disallowed normal harmonics, followed by still smaller skew harmonic terms which are also symmetry disallowed. This pattern can frequently be observed in the RMS of values for a given set of magnets. This effect is apparent in the odd-even (parity) differences in Figure 12 but is not obvious in the tables above. Instead, the set of graphs from which Figure 11 is selected revealed a pattern in which the highest order term had significant variations which propagated to other terms of the same parity. As with the other considerations above, this suggests that, although the polynomials do fit the observed field shape, their averages or their use as harmonics (representing the two dimensional rather than only the one dimensional field shape) should be only as limits for terms other than the quadrupole and sextupole.

Many authors have shown that for dipoles of rectangular cross section, the error fields (such as those from coil placement), which are induced at the edge of the aperture, fall off as a sum of exponential terms when one approached the center of the magnet. This is related to the solution of Laplace's Equation in rectangular coordinates which is most compactly represented in terms of products of hyperbolic and circular sinusoids. We should not be surprised then, that an examination of the magnitude of polynomial

fit coefficients, when examined as a function of fit width, will also fall off exponentially. Nevertheless, the polynomials do provide a useable description of the measured field on the midplane. What needs to be explained in light of these 'natural' exponential behaviors, is the uniform sextupole field observed. The magnets, when powered to 1180 A, have saturated the iron and begun to show non-uniformities associated with saturation. The geometric scale of these is set by the transverse size of the yoke and the coil separation.

The regularities of the field shape of these magnets is easy to characterize. The dipole is modified by a sextupole of 20 parts per million at an inch which is nearly uniform over the central ± 3 inches of the aperture. The quadrupole consists of a term of about 36 parts per million at an inch at $x = 0$ as measured by FLATCOIL, to which one must add an end field contribution. In the central region of this magnet other terms are still smaller.

The differences between magnets LDA001-LDA010 on the one hand and LDA011 through LDA013 on the other hand, although small on an absolute scale, remain very significant in light of the uniformity of the rest of the set. Examination of the reported errors, which would reveal differences between the three passes of the probe, show the measurements of these magnets to be typical. We have only one measurement of LDA011 but additional measurement of LDA012 and LDA013 confirm the reported field shape. We have found no comment concerning these small shape differences from the period when they were built, measured, reviewed and installed.

Finally, to display the uniformity of these fields, we present Figure 13 in which we again present the measured shape with the contributions from the dipole, quadrupole and sextupole terms subtracted. We have done this at both the magnet center ($x = 0$) and at a position near the antiproton core. Over a range which is large compared the the beam size due to transverse emittance and betatron motion, we have field errors of a few parts per million.

4 Acknowledgements

This work was the result of a large effort on the part of many people. We cannot properly thank them all here, but we would like to make several acknowledgements. The staff of the development group at MTF and of the TeV I magnet group provided the measurement hardware and software used in this effort. The MTF measurement staff provided faithful execution of

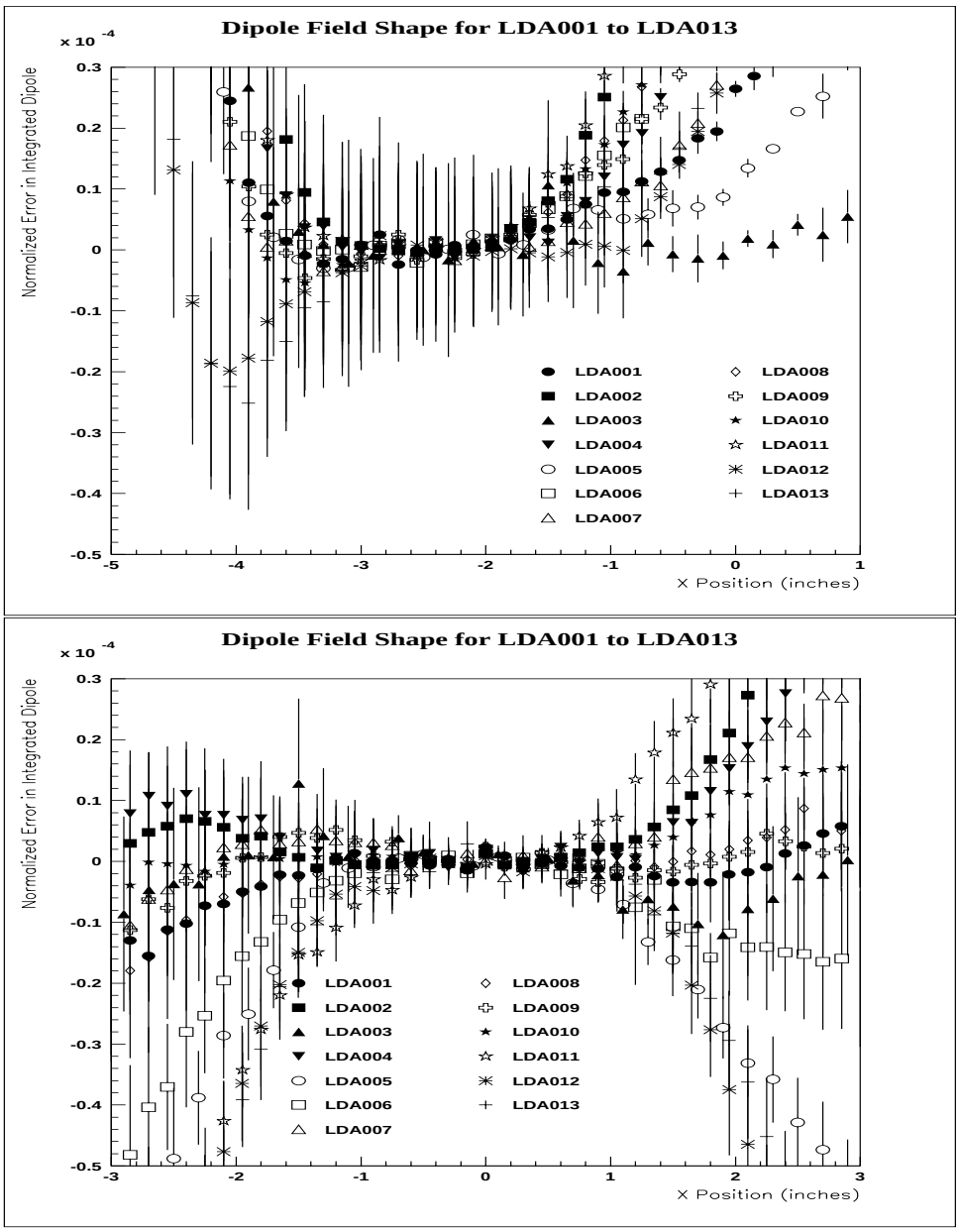

Figure 13: The field shape data presented at high resolution after subtraction of low order harmonics. We plot $s(x) - b_1 - b_2 x - b_3 x^2$ *vs.* x for all the magnets. Upper plot uses individual magnet harmonics fit about center at -2.5 inches. Lower plots uses fit about center at $x = 0$. Fit width parameter used is 1.95 inches, which will include data to ± 2 inches.

the prescribed measurement procedures. I would like to acknowledge the 10 years of effort by Julian Plymale and others at MTF responsible for preserving access to this data. Paul Mantsch at MTF and John Peoples in the TeV I project provided supportive leadership for the measurement effort. In addition, John Peoples provided the encouragement to reexamine this data during discussions of the proposed Fermilab Recycler Ring in July 1995. Discussions with John Marriner, Mike Church, Phil Martin, Dave Harding, and Shekhar Mishra were particularly helpful in understanding accelerator issues. Hank Glass and Dana Walbridge provided help with PAW. Dave Harding reviewed the manuscript. Finally, I would like to acknowledge the physicists who assisted in prescribing, assembling and operating these measurement systems: Dave Harding, Arlene Lennox, Peter Mazur, Fred Mills, Bob Peters, and Alan Wehmann.

References

[1] Design Report Tevatron 1 Project, September 1983.

[2] B. C. Brown, D. J. Harding, M. F. Gormley, M. E. Johnson, A. J. Lennox, K. J. McGuire, J. E. Pachnik, J. K. Plymale, R. A. Shenk, and A. A. Wehmann. Data Acquisition System Design for Production Measurements of Magnets for the Fermilab Anti-Proton Source. *IEEE Trans. on Nuc. Sci*, NS-32:2050, 1985.

[3] H.D. Glass, B. C. Brown, J. DiMarco, D. J. Harding, P. O. Mazur, C. S. Mishra, A. Mokhtarani, D. F. Orris, C. M. Reid, J. W. Sim, J. C. Tompkins, and D. G. C. Walbridge. Flatcoil Systems for Measurements of Fermilab Magnets. to be published in Proceedings of 14th International Conference on Magnet Technology. Available as FERMILAB-CONF-95-143.

[4] Henry D. Glass. Measurement of Harmonic Amplitudes and Phases Using Rotating Coils. Technical Report MTF-94-0004 1.1, Fermilab, March 1994.

A Measurement Hardware

The measurement system[2] for the TeV I dipoles used a VAX 11/730 with a serial CAMAC interface to control hardware for the measurement systems.

A Measurement Station consisted of a CAMAC crate for control and data acquisition modules, DVM's controlled and read by GPIB, and various other control and interface modules. Magnets were mounted on Stands that were equipped with alignment systems, x-y translation tables (with x motion automated and read by computer) and a 150 kW PEI power supply. The measurements of the heaviest dipoles (LDA, SDA, SDB) in the TeV I project were carried out at Fermilab's B0 Assembly Building. Measurement Stations there were interfaced to the VAX11/730 over a fiber optic CAMAC link. LDA Dipoles were measured using Stand F and Measurement Station A4.

The Flatcoil probes for TeV I dipoles used a coil form of 0.25 inch wide extruded Aluminum. For LDA (15 foot), SDA(15 foot) , and SDB(10 foot) dipoles, the measurement coils used were 19 ft long. On this a simple coil with 10 turns of Copper wire were wound.[5] This form was bent to conform to the magnet curvature, so that the probe measured directly the field experienced by a particle. The coil form was mounted in an extruded aluminum box which was mounted on wheels. These wheels rode on the surface of the lower poletip laminations and elevated the coil to be on the vertical symmetry plane of the magnet. In order to scan the field shape in the horizonal plane, the coil was moved by rolling the wheels on the poletip. The Aluminum box of the probe body was reinforced using a carbon fiber layup. The boxbeam and carbon fiber assembly was bent to the desired radius and cured to maintain the desired shape.

The probe ends were held with a fixture mounted on a cross-slide pair which provided x (horizonal) and y (vertical) adjustment. The x motion was driven using a stepping motor and the x position was read with a standard incremental position encoder based on the chrome-on-glass technique with an encoder line spacing of 0.001 inch. The resulting position errors are ignorable.

Measurements were performed without the beam chamber in place. Therefore, despite the size of the FLATCOIL probe, the coil form was able to scan over almost the entire horizonal aperture which is available to the beam. The transverse (x) direction was selected to be perpendicular to the beam orbit at the longitudinal center of the magnet. The y direction points up and the

[5]The data analysis will assume that the flux deviation measured at each x position is to be related to the local field (dipole) at that location. In fact, for a probe of finite width, one can relate the flux observed at a point to a sum of terms each of which is the product of a harmonic expansion coefficient and a probe sensitivity coefficient (see Glass[3]). For this probe system, the sextupole and small higher order terms can be ignored for measurements of magnets such as the LDA's.

x direction points in the radially outward direction for the storage ring. The magnets were powered with the B Field pointed up ($B_y > 0$). Since these dipoles are not sector magnets, but instead have each end parallel to x direction described above, they have a quadrupole endfield contribution to the integrated field seen by the beam. This contribution will not be measured by the FLATCOIL measurement system.

The changes in magnetic flux experienced by the probe were integrated using a conventional analog integrator based on a chopper-stabilized operational amplifier (AD 234L) read by a Digital Volt Meter (DVM). Resolution is limited by the input noise of the operational amplifier. Manual switching systems were used to configure various coil combinations but all critical switch positions were recorded by the data acquisition system to confirm that the selected measurement configuration corresponded to the configuration assumed for analysis.

B Data Collection and Reduction

A sequence of self-contained measurement runs acquired the data and reduced that data to engineering units, accounting for the peculiarities of the measurement sequence and hardware calibrations. Raw data was recorded to a disk file per run with minimal calibration and correction applied. Data reduction applied calibrations to account for the conversion constants for the specific hardware in use and corrected for the integrator drift and other limitations of the measurement system. Reduced data was then recorded to a disk file on a per run basis, ready for further analysis.

LDA measurements were performed with the TEST magnet connected in series with a REFerence magnet. By installing a second 19 foot flatcoil in the reference dipole and connecting it in a passive differencing circuit, one could measure the difference in flux change between the two probes. Measurements with the Test coil alone are designated MEAS (M) runs, with the reference coil alone REF (R) runs and with the difference (MEAS - REF) designated BUCK (B). The field shape data we are reporting were recorded using the BUCK configuration.

FLATCOIL systems implemented with curved probes can obtain magnet strength information by measuring the flux changes induced by ramping the magnet. This was done for each of the configurations (M,R,B) on each magnet. We will use the MEAS results to normalize shape measurements. The strength measurements were designated as BASELINE (B) runs and

were taken by centering the probe in the magnet, ramping the magnets thru a series of ramps to establish hysteresis, then measuring flux at 0 A excitation (usually three times), exciting to nominal current and recording the integrated flux change (usually three times) and then ramping to 0 A and recording the flux (a final three times). After saving these results, the data was reduced by converting the observed voltages to flux and fitting the measured fluxes at several times and two excitation levels to the assumption that the flux is linear in time and current[6] The coefficient for the term linear in current is recorded as the SLOPE and is the strength output from this measurement. By multiplying the SLOPE by the nominal (requested) current for the excitation, one obtains a strength measure at a given current for the magnet. SLOPE is recorded in flux change per ampere (volt-seconds/ampere) since the calibration (effective width) of the probe was not essential to either the shape or the relative strength of the magnets under test. A precise calibration of the probe is still not available.

Shape measurement runs begin by centering the the probe in the magnet and then exciting the dipole with a series of hysteresis ramps, followed by a ramp to the desired current. The probe was then rolled to the desired limit in -x and the analog integrator was reset. At that point and each succeeding point, several (usually 3) data points were recorded consisting of a time stamp, a measured flux and a measured current. The the probe was moved one step in x and the data recorded (with the probe stationary) for that location. First pass data collection continued stepwise until the symmetric +x limit was reached. The second pass stepped from +x limit back to the -x limit while the third pass recorded data at the same point sequence as pass one. The data reduction algorithm determined the integrator offset (drift) using 10 points adjacent to x=0 and fitting them to obtain linear and quadratic drift terms. Shape data were then recorded as flux change (corrected for drift) divided by measured current[7] The desired shape information

[6]This very limiting assumption which had been specified for the analysis required that obtaining measurements at different excitation levels were done using a series of runs. In that case, after each measurement at nominal current, one ramped to the peak of the hysteresis ramp for the measurement before ramping to 0 A. Note that with the precision of measurement achieved in this system, ($> 3 \times 10^{-4}$) virtually all magnets are not linear in excitation.

[7]Current changes were very small and were cancelled in the measured flux by the reference coil. So, despite the fact that one might believe that a correction based on the change in current was more appropriate that one based on dividing by the current, it is not a material consideration. The algorithm implemented was the one specified for the project.

should be normalized to the measured field integral from a BASEline run. For measurements taken with an integrating scan, the error analysis is a bit subtle for most measurement sequences. The errors recorded for the shape are the simply the RMS of the flux change per ampere determination from the three passes with no attempt to remove the correlated errors between points. See discussion in Section 2.

C Effects of Fit Widths

The prejudice to fit magnet harmonics to within a radius less than the minimum pole tip radius derives from the fact that within such a radius we are guaranteed to have a suitable expansion by solid mathematical arguments. If one extends beyond the maximum radius which is contained within the matter-free region, one cannot guarantee that a harmonic expansion will converge. In fact, the use of a larger radius will not necessarily result in a non-convergent series, but one often uses that radius to avoid considering special cases and/or unproductive discussions with colleagues. Such arguments do not directly guide the fitting for the polynomial fits used in this report.

The considerations of local traditions combined with the desire to maximize the range over which fitted harmonics were reported guided the initial selection of a ± 1 inch fit range for the body of this paper. However, an examination of the apparent higher order field contributions in a plot which suppressed individually fitted quadrupole and sextupole harmonics produced a concern that the fit range was not optimal. The data in question is shown in the upper portion of Figure 14. When comparing this data to that in Figure 3, we see that the average sextupole seems to better fit the data at larger ranges than the individual fits over a ± 1 range. If fits to larger ranges are used to establish the sextupole fields, using only up to 16-pole (x^7) terms, we find that no range is obviously optimal. This is illustrated in Figures 14 and 15. These considerations provided essential clues to the fitting problems discussed in Section 2.4.

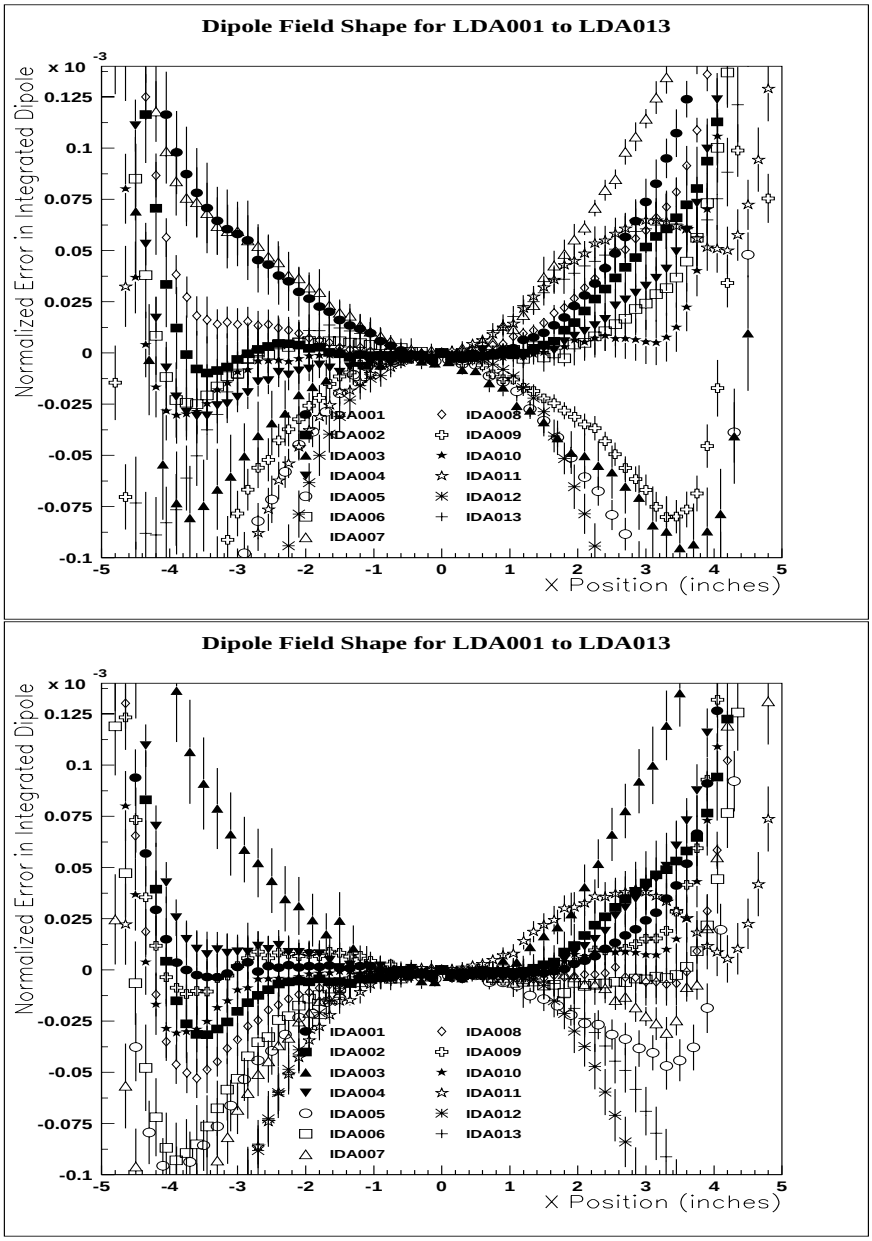

Figure 14: Scan data with fitted quadrupole and sextupole term subtracted. Fit width of ± 1 inch was used for the upper plot while fit width of ± 1.5 inch was used for the lower plot.

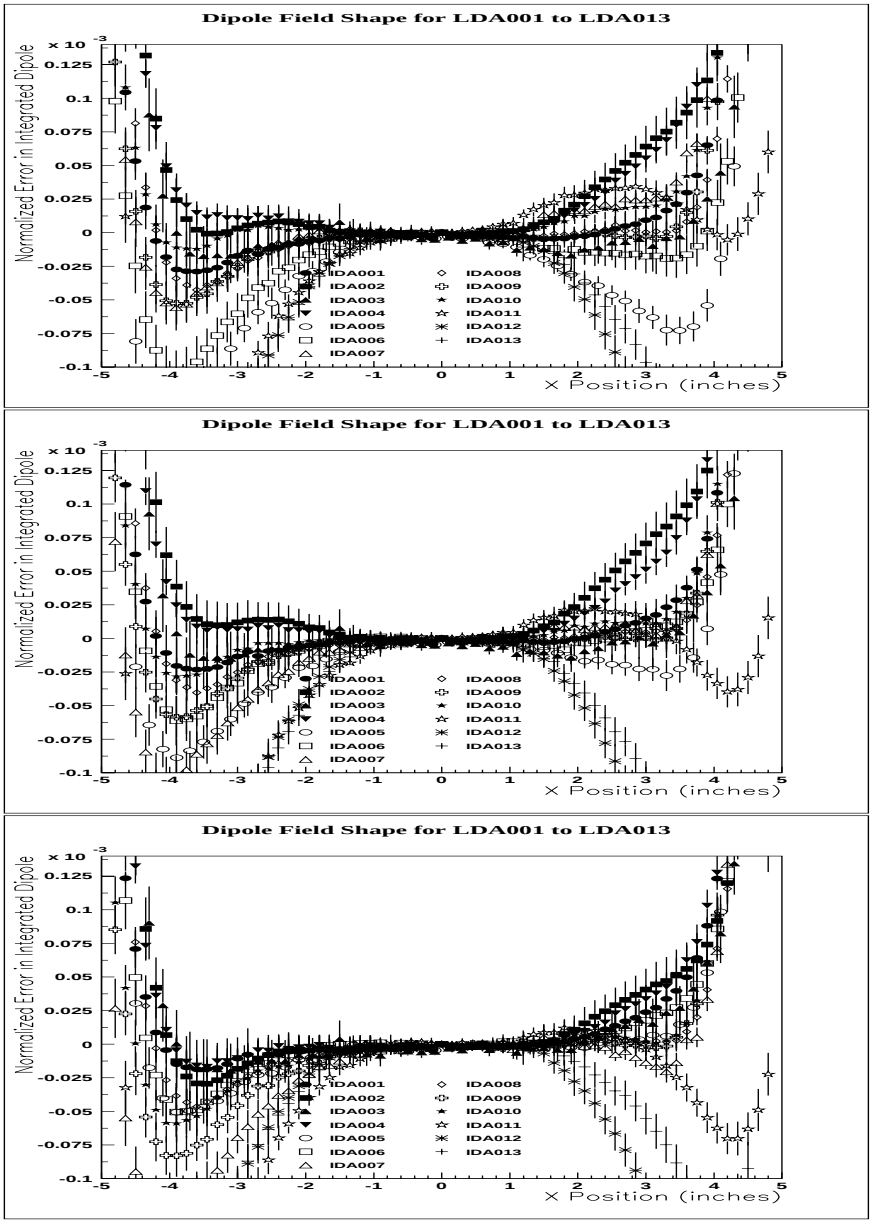

Figure 15: Scan data with fitted quadrupole and sextupole term subtracted. Fit widths of ± 2, ± 2.5, ± 3.4 inch were used for top, middle, and bottom figures respectively.